



HAL
open science

Structure of optimal control for planetary landing with control and state constraints

Clara Leparoux, Bruno Hérissé, Frédéric Jean

► **To cite this version:**

Clara Leparoux, Bruno Hérissé, Frédéric Jean. Structure of optimal control for planetary landing with control and state constraints. ESAIM: Control, Optimisation and Calculus of Variations, 2022, 28, 10.1051/cocv/2022065 . hal-03642339

HAL Id: hal-03642339


<https://ensta-paris.hal.science/hal-03642339>

Submitted on 5 Mar 2024

HAL is a multi-disciplinary open access archive for the deposit and dissemination of scientific research documents, whether they are published or not. The documents may come from teaching and research institutions in France or abroad, or from public or private research centers.

L'archive ouverte pluridisciplinaire **HAL**, est destinée au dépôt et à la diffusion de documents scientifiques de niveau recherche, publiés ou non, émanant des établissements d'enseignement et de recherche français ou étrangers, des laboratoires publics ou privés.

STRUCTURE OF OPTIMAL CONTROL FOR PLANETARY LANDING WITH CONTROL AND STATE CONSTRAINTS

CLARA LEPAROUX^{1,2}, BRUNO HÉRISSE¹ AND FRÉDÉRIC JEAN^{2,*} 

Abstract. This paper studies a vertical powered descent problem in the context of planetary landing, considering glide-slope and thrust pointing constraints and minimizing any final cost. In a first time, it proves the Max-Min-Max or Max-Singular-Max form of the optimal control using the Pontryagin Maximum Principle, and it extends this result to a problem formulation considering the effect of an atmosphere. It also shows that the singular structure does not appear in generic cases. In a second time, it theoretically analyzes the optimal trajectory for a more specific problem formulation to show that there can be at most one contact or boundary interval with the state constraint on each Max or Min arc.

Mathematics Subject Classification. 49N60, 49K15, 49N90.

Received May 11, 2022. Accepted October 5, 2022.

1. INTRODUCTION

Interest for vertical landing problems has increased these recent years with the growing use of reusable launchers and as space exploration missions are requiring ever more landing precision. Vertical landing consists of two phases: first an entry phase, that set the vehicle in appropriate position and velocity conditions above the target to ensure landing feasibility, and then a phase of powered descent. Prior to the powered descent, the reference trajectory has to be recalculated in order to correct dispersions accumulated during the entry phase as explained in [4], or to handle an update of the landing site ([12]). This motion planning problem is usually treated in an optimal control framework, as stated originally in [15], allowing to minimize a quantity such as fuel consumption, flight time, or landing errors to ensure soft landing. More particularly, within the framework of Mars Science Laboratory missions, [19] and [16] argue on the benefit of pinpoint landing guidance strategies, consisting in solving an optimal control problem minimizing fuel consumption under the constraint of reaching the target exactly. Indeed, this formulation is consistent with the requirements of the former Mars missions which asked an extreme landing precision despite the difficulties of estimating the position accurately on Mars [25], with an heavy payload making fuel saving vital to permit retargeting.

However, solving an optimal control problem efficiently and accurately remains a challenge [23]; moreover, analytical solutions, computed thanks to the Pontryagin Maximum Principle, are only known for simplified models with few constraints, as in [2] and [11]. For the particular case of control-affine dynamics, [20] and [18]

Keywords and phrases: Optimal Control, Aerospace, Planetary Landing.

¹ DTIS, ONERA, Université Paris-Saclay, 91123 Palaiseau, France.

² UMA, ENSTA Paris, Institut Polytechnique de Paris, 91120 Palaiseau, France.

* Corresponding author: frederic.jean@ensta-paris.fr

showed that optimal controls consist of a finite concatenation of arcs on which the control norm is constant and arcs on which the control is singular. This paper is concerned with the following dynamic model, expressed in an inertial frame (e_x, e_y, e_z) ,

$$\begin{cases} \dot{r} &= v, \\ \dot{v} &= \frac{T}{m}u - g, \\ \dot{m} &= -q\|u\|, \end{cases} \quad (1.1)$$

where $r(t) = (x(t), y(t), z(t)) \in \mathbb{R}^3$ is the vehicle position, $v(t) \in \mathbb{R}^3$ is its velocity, $m(t) > 0$ is its mass, q the maximal mass flow rate of the engine, $T > 0$ the maximal thrust and $g = (0, 0, g_0)$ with g_0 the gravitational acceleration. The thrust is controlled by the vector $u(t) \in \mathbb{R}^3$, where $\|u\| \leq 1$ is the engine throttle. Previous theoretical and numerical studies tend to show that the structure of the optimal control for dynamics equation (1.1) generally does not contain singular arcs. Indeed, [6] shows the Bang-Bang characteristic of controls minimizing a L^1 -norm. In the case of landing, [13] has first showed that the optimal control of the one dimension fuel-optimal problem with a bounded control follows an Off-Bang structure, *i.e.* it has a period of off thrust followed by full thrust until touchdown. Then, the Bang-Off-Bang structure, called Max-Min-Max when the thrust is not allowed to go to zero, has been found to be optimal for numerous variants of the problem, such as the two-dimensional problem studied in [9], the problem with specified initial and final thrust studied in [21], or with throttle and thrust angle control in [22]. Recently, [8] and [14] showed that the Max-Min-Max structure is the solution of the one dimension problem, minimizing the final time for the first one and considering the effect of an atmosphere on the thrust for the latter. More generally, considering the problem of controlling a vehicle in space but not necessarily during the landing phase, [17] shows that the optimal control is a finite succession of Min and Max arcs. However, there lack theoretical studies relating more complex formulations of the landing problem, for instance considering realistic technical and safety constraints. Among the existing numerical methods, a noteworthy one is presented in [1, 2, 5], that succeeds to solve efficiently the problem including constraints on the thrust direction and the launcher position, thanks to a convexification method. The simulations carried out in these studies also reveal a Max-Min-Max form of control.

The purpose of this paper is to analyze a vertical landing problem considering relevant control and state constraints to highlight the rigidity of the solution. Indeed, we show that the structure of the control remains identical after changing the cost or adding constraints, which suggests that it is not specific to the problem formulation (we can even modify the dynamic model to take into account the effect of an atmosphere). We will study at first the problem with dynamics equation (1.1) and we will consider, in addition to the bound on the control norm, a thrust pointing constraint limiting the amplitude of the control direction as well as the launcher orientation, both for safety reasons and to model actuator limitations. Then, we also take into account a glide-slope constraint, forcing the launcher position to stay inside a cone centered on the target, to ensure that the vehicle remains at a safe altitude and to guarantee sensor operability. The cost of the optimal control problem considered is expressed as a final cost, which embraces the most common applications such as maximizing the final mass or minimizing the final time. Our main result is that, in this framework (defined later as Prob. 2.1), an optimal control has either a Max-Min-Max form or a Max-Singular-Max form as stated below.

Theorem 1.1. *Consider an optimal trajectory on $[0, t_f]$. Then, the control $u(t)$ is in the Max-Min-Max or the Max-Singular-Max form, *i.e.* there exist t_1 and t_2 with $0 \leq t_1 \leq t_2 \leq t_f$ such that*

$$\|u(t)\| = \begin{cases} u_{\max} & \text{if } t \in [0, t_1] \cup (t_2, t_f], \\ u_{\min} \text{ or singular} & \text{if } t \in [t_1, t_2]. \end{cases}$$

Remark 1.2. When $t_1 = 0$ or $t_2 = t_f$, the Max-Min-Max or Max-Singular-Max form degenerates in a Max, Min, Singular, Max-Min, Max-Singular, Min-Max or Singular-Max form.

Moreover, ignoring the pointing constraint, we show that the optimal controls keep the same structure when considering the effect of the atmosphere on the thrust force at low altitude (the pressure is assumed to be constant with respect to altitude).

We then complete the analysis of optimal trajectories by studying two types of sub-arcs that play a particular role both from a theoretical and a numerical point of view, namely singular arcs and boundary arcs (where the state constraint is active). We show that singular arcs rarely occur, and that at most three boundary arcs appear in an optimal trajectory, the latter result being proved only in a particular case. Besides, the numerical results available make think that this outcome is likely to be generalized. Note that some of the above results have already been stated in the conference paper [10] but without most of the demonstrations, all details are given here.

The paper is organized as follows. In Section 2, the full optimal control problem with the constraints considered is presented, and the optimality conditions given by application of PMP are detailed. Section 3 is devoted to the proof of Theorem 1.1 and to its extension to the case with a model of the atmosphere. Section 4 studies the singular arcs and the number of contact points with the state constraint. Finally, Section 5 provides numerical results.

2. PROBLEM STATEMENT

2.1. Formulation

We consider vehicles with dynamics in the form of equation (1.1), whose state is denoted by $X = (r, v, m) \in \mathbb{R}^3 \times \mathbb{R}^3 \times \mathbb{R}$. It is subject to the following constraints:

- bounds on the control norm,

$$u_{\min} \leq \|u\| \leq u_{\max},$$

- a pointing constraint (Fig. 1), formulated as

$$\langle e_z, u \rangle \geq \|u\| \cos(\theta), \text{ where } \theta \in [0, \frac{\pi}{2}) \text{ is a constant,}$$

- a glide-slope constraint (Fig. 2),

$$h(r) = z - \tan(\gamma)\|(x, y)\| \geq 0, \text{ where } \gamma \in [0, \frac{\pi}{2}) \text{ is a constant,}$$

- a mass constraint,

$$m \geq m_e, \text{ where } m_e > 0 \text{ denotes the empty mass of the vehicle.}$$

The landing problem consists in reaching a target on the ground (zero terminal altitude and vertical velocity) while minimizing a final cost. The target and the cost are chosen as follows.

- We represent the target as a subset $\mathcal{C} \subset \mathbb{R}^7$ to which the final state $X(t_f)$ must belong. This set is designed so that the final state has zero terminal altitude and vertical velocity, and is close to $r = 0$ and $v = 0$ ($r = 0$ represents the center of the physical target here). It should at least satisfy the following property,

$$\{X \in \mathbb{R}^7 : r = v = 0\} \subset \mathcal{C} \subset \{X \in \mathbb{R}^7 : z = v_z = 0\}. \quad (2.1)$$

- The terminal cost $\ell(t, X)$ usually penalizes the total duration (minimal time problems) or the diminution of the mass (maximisation of the final mass). It may also contain a penalization of the final horizontal positions and velocities (in the case where the target \mathcal{C} does not ensure that these quantities are small

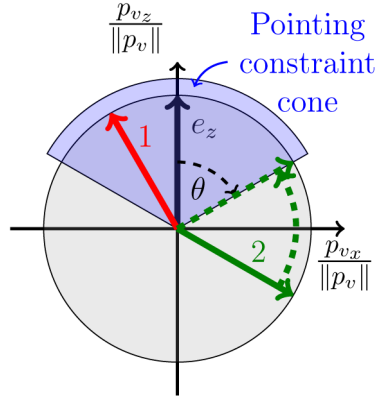


FIGURE 1. The thrust pointing constraint. Red: nonsaturating orientation. Green: saturating orientation.

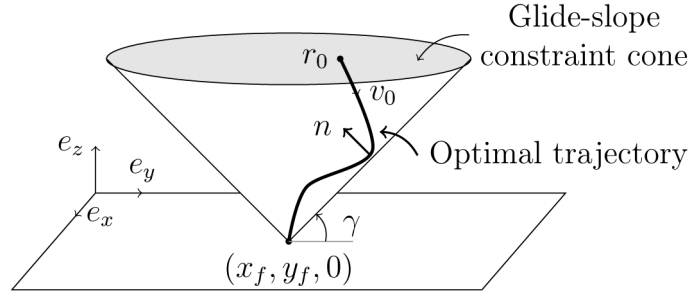


FIGURE 2. Glide-slope constraint.

at the final state). We summarize this by imposing that ℓ is a C^1 function which satisfies, for every $t \in (0, +\infty)$ and $X \in \mathbb{R}^7$,

$$\frac{\partial \ell}{\partial t}(t, X) \geq 0, \quad \frac{\partial \ell}{\partial m}(t, X) \leq 0, \quad \ell(t, (r = 0, v = 0, m)) \leq \ell(t, X). \quad (2.2)$$

To summarize, the landing problem can be written as the following optimal control problem in free time.

Problem 2.1.

$$\min \ell(t_f, X(t_f)) \text{ such that } \begin{cases} X(\cdot) = (r(\cdot), v(\cdot), m(\cdot)) \text{ follows equation (1.1),} \\ X(0) = (r_0, v_0, m_0), \\ X(t_f) \in \mathcal{C}, \\ m(t) > m_e \forall t \in [0, t_f], \\ u_{\min} \leq \|u\| \leq u_{\max}, \\ \langle e_z, u \rangle \geq \|u\| \cos(\theta), \\ h(r) \geq 0. \end{cases}$$

Remark 2.2. The mass constraint $m(t) = m_e$ cannot be reached for $t \in [0, t_f]$. Indeed it would imply that $u = 0$ on $[t, t_f]$, which makes it impossible to reach $z(t_f) = 0$ with $v_z(t_f) = 0$. Thus, the mass constraint writes as a strict inequality $m(t) > m_e$ and it plays no role in the optimality conditions.

Remark 2.3. If there exists trajectories $X(\cdot)$ satisfying the constraints of Problem 1, then this problem admits optimal solutions, it results from an adaptation of the results in [2]. Indeed, the existence is proved in [2] for the same problem formulation but without considering the pointing constraint. The proof consists in first convexifying the constraints and then showing the existence of an optimal solution for the convex formulation of the problem ([2], Thm. 1). The second part of the reasoning still works when we add the convexified pointing constraint. Then, it is necessary to show that optimal solutions of the convexified problem are also optimal for the nonconvex formulation of the problem. This is done in ([2], Lem. 2) without the pointing constraint, and in ([1], Lem. 1) when considering the pointing constraint.

2.2. Optimality conditions

We give in this section the necessary optimality conditions provided by the Pontryagin Maximum Principle applied to the optimal control Problem 2.1. Let us firstly specify some notations.

- For $p = (p_x, p_y, p_z) \in \mathbb{R}^3$, we set $\bar{p} = (p_x, p_y)$.
- The glide-slope constraint writes as $h(r) = r_z - \tan(\gamma)\|\bar{r}\|$. At a point r such that $\bar{r} \neq 0$ the gradient of h is

$$n := \nabla h(r) = \begin{pmatrix} -\tan(\gamma) \frac{\bar{r}}{\|\bar{r}\|} \\ 1 \end{pmatrix}.$$

- The control set is $\mathcal{U} = \{u \in \mathbb{R}^3 : u_{\min} \leq \|u\| \leq u_{\max} \text{ and } \langle e_z, u \rangle \geq \|u\| \cos(\theta)\}$.

Since the glide-slope constraint is a state constraint, we need a version of the maximum principle able to take into account such constraints. We choose the one given in Theorem 9.5.1 of [24], which in our case writes as follows. Define the Hamiltonian of Problem 2.1 as

$$H(X, P, u) = \langle p_r, v \rangle + \langle p_v, \frac{T}{m}u - g \rangle - p_m q \|u\|, \quad (2.3)$$

where the adjoint vector $P = (p_r, p_v, p_m)$ belongs to $\mathbb{R}^3 \times \mathbb{R}^3 \times \mathbb{R}$.

Let $(X(\cdot), u(\cdot))$ be an optimal solution of Problem 2.1. Then there exists a constant $p^0 = 0$ or -1 , an absolutely continuous function $P(\cdot)$ on $[0, t_f]$, and a nonnegative Borel measure μ on $[0, t_f]$, such that, writing

$$Q(t) = (q_r(t), p_v(t), p_m(t)), \quad q_r(t) = p_r(t) - \int_{[0,t)} n(s)\mu(ds), \quad (2.4)$$

we have:

1. $(P, p^0, \mu) \neq (0, 0, 0)$;
2. $\text{supp}\{\mu\} \subset \{t \in [0, t_f] : h(r(t)) = 0\}$;
3. (dynamics of the adjoint vector) for a.e. $t \in [0, t_f]$,

$$\begin{cases} \dot{p}_r(t) &= 0, \\ \dot{p}_v(t) &= -q_r(t), \\ \dot{p}_m(t) &= \frac{T}{m(t)^2} \langle p_v(t), u(t) \rangle; \end{cases}$$

4. (maximization condition) for a.e. $t \in [0, t_f]$,

$$H(X(t), Q(t), u(t)) = \max_{w \in \mathcal{U}} H(X(t), Q(t), w);$$

5. (transversality condition)

$$\max_{w \in \mathcal{U}} H(X(t_f), Q(t_f), w) = -p^0 \frac{\partial \ell}{\partial t}(t_f, X(t_f)). \quad (2.5)$$

Note that we omit the terminal conditions on $Q(t_f)$ since we do not need them.

Remark 2.4. When $\gamma \neq 0$, the function h is not differentiable at points r with $\bar{r} = 0$ and its gradient n is not defined at such points. Thus, following the notations of [24], we should write $q_r(t)$ in equation (2.4) as

$$q_r(t) = p_r(t) - \int_{[0,t)} \partial^> h(r(s)) \mu(ds),$$

where $\partial^> h$ denotes a partial subdifferential. However this expression coincides with the one of equation (2.4) since at an interior time $s \in (0, t_f)$ where $\mu \neq 0$, *i.e.* $h(r(s)) = 0$, $\bar{r}(s)$ is nonzero. Indeed, otherwise $h(r(s)) = 0$ would imply $r(s) = 0$ since $\gamma \neq 0$, and then $v_z(s) = 0$, as z has reached a minimum. Then, as near s there holds $z(t) = o(t - s)$ and $h(t) = -\tan(\gamma)|t - s| \|\bar{v}(s)\| + o(t - s)$, $h(t) \geq 0$ would imply that $\bar{v}(s) = 0$, and thus $r(s) = v(s) = 0$. Hence $X(s)$ would belong to the target \mathcal{C} by equation (2.1) and minimize the cost ℓ by equation (2.2), a contradiction with $s < t_f$.

3. STRUCTURE OF OPTIMAL CONTROLS

3.1. Solution of the optimal control problem

We first exploit equations of the Pontryagin Maximum Principle to obtain information on the evolution of the control. Those results will be necessary to deduce the general form of the control with respect to time.

For $d = 1, 2$, we denote by \mathcal{S}^d the unit sphere in \mathbb{R}^{d+1} . Remind also that, for $p_v = (p_{v_x}, p_{v_y}, p_{v_z})$, we set $\bar{p}_v = (p_{v_x}, p_{v_y})$.

Lemma 3.1. *Let $u(t)$, $t \in [0, t_f]$, be an optimal control of Problem 2.1, and $P(\cdot)$ be its adjoint vector. Then, for any $t \in [0, t_f]$ such that $u(t) \neq 0$, there holds*

$$\frac{u(t)}{\|u(t)\|} = d(t),$$

where $d : [0, t_f] \rightarrow \mathcal{S}^2$ is a measurable function satisfying

$$d(t) = \begin{cases} \frac{p_v(t)}{\|p_v(t)\|} & \text{if } p_{v_z}(t) \geq \|p_v(t)\| \cos(\theta) \text{ and } p_v(t) \neq 0, \\ \left(\sin(\theta) \frac{\bar{p}_v(t)}{\|\bar{p}_v(t)\|}, \cos(\theta) \right) & \text{if } p_{v_z}(t) < \|p_v(t)\| \cos(\theta) \text{ and } \bar{p}_v(t) \neq 0, \\ \left(\sin(\theta) \delta, \cos(\theta) \right) \text{ with } \delta \in \mathcal{S}^1 & \text{if } p_{v_z}(t) < \|p_v(t)\| \cos(\theta) \text{ and } \bar{p}_v(t) = 0. \end{cases}$$

Moreover, set

$$\Psi(t) = \frac{T}{m} \langle p_v(t), d(t) \rangle - p_m(t)q, \quad t \in [0, t_f].$$

Then we have

$$\|u(t)\| = \begin{cases} u_{\max} & \text{if } \Psi(t) > 0, \\ u_{\min} & \text{if } \Psi(t) < 0. \end{cases}$$

Proof of Lemma 3.1. If $u(\cdot)$ is an optimal control on $[0, t_f]$, then the maximization condition of the Pontryagin Principle implies that, for almost all $t \in [0, t_f]$, $u(t)$ maximizes

$$\varphi(t, w) = \langle p_v, \frac{T}{m}w \rangle - p_m q \|w\|$$

among the $w \in \mathcal{U}$. Making the change of variable $w = \alpha d$, with $\alpha = \|w\|$ and $d \in \mathcal{S}^2$, to find $u(t) \in \mathcal{U}$ maximizing φ amounts to find α and d maximizing

$$\varphi(t, w) = \alpha \left(\frac{T}{m} \langle p_v, d \rangle - p_m q \right)$$

under the conditions $u_{\min} \leq \alpha \leq u_{\max}$ and $d \in \mathcal{D} = \{d \in \mathcal{S}^2 : \langle e_z, d \rangle \geq \cos(\theta)\}$. Let us write

$$\varphi(t, w) = \alpha \psi(t, d), \quad \text{where} \quad \psi(t, d) = \frac{T}{m} \langle p_v, d \rangle - p_m q.$$

First, $\alpha \geq 0$ implies that

$$\max \varphi = \max_{\alpha} \left[\alpha (\max_d \psi) \right].$$

Then, the maximum of φ is attained for α satisfying

$$\begin{cases} \alpha = u_{\max} & \text{if } \max(\psi) > 0, \\ \alpha = u_{\min} & \text{if } \max(\psi) < 0, \end{cases}$$

and for d solution of the problem

$$\max_d \psi = -p_m q + \frac{T}{m} \max_{d \in \mathcal{D}} \langle p_v, d \rangle.$$

It is a matter of an exercise to check that the solution d of this maximization problem satisfies the statement of the lemma (for the sake of completeness we give the proof in Appendix, in Lem. A.1). Lemma 3.1 follows by setting $\Psi = \max_d \psi$. \square

Thus, the norm of the control is mainly determined by the sign of the switching function Ψ and takes only the values u_{\min} and u_{\max} when Ψ is nonzero (*bang arcs*). Therefore, we need to analyze the variations of Ψ , which we will do now. Note however that, on time intervals where Ψ is zero, the value of the control cannot be deduced directly from the maximisation of the Hamiltonian. Such parts of the trajectory are called *singular arcs*, they are the subject of a further study in Section 4.1.

Remark 3.2. The direction d of the control is more regular than just measurable. Indeed let $I \subset [0, t_f]$ be the closed set such that, for every $t \in I$,

$$p_v(t) = 0 \quad \text{or} \quad p_{v_z}(t) < 0 \quad \text{and} \quad \bar{p}_v(t) = 0.$$

Equivalently, for every $t \in [0, t_f] \setminus I$, there holds

$$p_v(t) \neq 0 \quad \text{and} \quad \text{if } p_{v_z}(t) < \|\bar{p}_v(t)\| \cos \theta, \quad \text{then } \bar{p}_v(t) \neq 0, \quad (3.1)$$

which implies that for these times $d(t)$ is defined as a function of $p_v(t)$. This function being locally Lipschitz, the function $d(\cdot)$ is absolutely continuous on every subinterval of $[0, t_f] \setminus I$. In particular $d(\cdot)$ is continuous on $[0, t_f] \setminus I$ while it may be discontinuous on I .

3.2. Variations of Ψ

Proposition 3.3. *Consider an optimal trajectory on $[0, t_f]$. Then:*

1. Ψ is absolutely continuous on $[0, t_f]$;
2. at a.e. $t \in [0, t_f]$, the time derivative of Ψ is

$$\dot{\Psi}(t) = -\frac{T}{m(t)} \langle q_r(t), d(t) \rangle; \quad (3.2)$$

3. $t \mapsto \langle q_r(t), d(t) \rangle$ is a nonincreasing function on a full measurement subset of $[0, t_f]$.

Proof of Points 1 and 2. Consider an optimal trajectory on $[0, t_f]$ with adjoint vector $P = (p_r, p_v, p_m)$. Recall that the switching function Ψ is given by

$$\Psi(t) = \frac{T}{m} \langle p_v(t), d(t) \rangle - p_m(t)q,$$

the function $d(\cdot)$ being defined in Lemma 3.1. Note first that, for every $t \in [0, t_f]$, there holds

$$\langle p_v, d \rangle(t) = \begin{cases} \|p_v(t)\| & \text{if } p_{v_z}(t) \geq \cos(\theta) \|p_v(t)\|, \\ \|\bar{p}_v(t)\| \sin(\theta) + p_{v_z} \cos(\theta) & \text{otherwise.} \end{cases}$$

Thus $\langle p_v, d \rangle$ is a Lipschitz function of p_v . Recall that the composition of a Lipschitz function with an absolutely continuous function is absolutely continuous (see [26], Ex. 9, p. 235¹). Since p_v is absolutely continuous on $[0, t_f]$, we deduce that $\langle p_v, d \rangle$ is absolutely continuous too, which proves Point 1.

Moreover, a simple computation shows

$$\dot{\Psi} = \frac{T}{m} \frac{d \langle p_v, d \rangle}{dt} \quad \text{a.e. on } [0, t_f],$$

so we are left with the computation of the time derivative of $\langle p_v, d \rangle$.

Let us introduce the subsets $I_1 = \{t \in [0, t_f] : p_v(t) = 0\}$, $I_2 = \{t \in [0, t_f] : \bar{p}_v(t) = 0 \text{ and } p_{v_z}(t) < 0\}$, and $I = I_1 \cup I_2$. As noticed in Remark 3.2, the function $d(\cdot)$ is absolutely continuous on $[0, t_f] \setminus I$. Hence $d(\cdot)$ is differentiable a.e. on this subset and we can compute directly the time derivative of $\langle p_v, d \rangle$ as follows:

- when the pointing constraint is not active, there holds $\langle p_v, d \rangle = \|p_v\|$ and then

$$\frac{d \langle p_v, d \rangle}{dt} = \frac{d \|p_v\|}{dt} = -\frac{\langle q_r, p_v \rangle}{\|p_v\|} = -\langle q_r, d \rangle.$$

- when the pointing constraint is active, $\langle p_v, d \rangle = \sin(\theta) \|\bar{p}_v\| + \cos(\theta) p_{v_z}$ and we obtain

$$\frac{d \langle p_v, d \rangle}{dt} = \sin(\theta) \left(\frac{-\langle \bar{q}_r, \bar{p}_v \rangle}{\|\bar{p}_v\|} \right) - \cos(\theta) q_z = -\langle q_r, d \rangle.$$

¹The reference is only an exercise, but its proof is elementary. It can be found for instance in Theorem 3.1 of the unpublished lecture notes of Jia Rong-Qing, [https://sites.ualberta.ca/~\\$sim\\$ria/Math418/Notes/chap3.pdf](https://sites.ualberta.ca/~simria/Math418/Notes/chap3.pdf).

As a consequence, equation (3.2) holds a.e. on $[0, t_f] \setminus I$.

Now, since $p_v = 0$ and $\langle p_v, d \rangle = 0$ on I_1 , we have $\dot{p}_v = -q_r = 0$ and $\frac{d\langle p_v, d \rangle}{dt} = 0$ a.e. on I_1 (see for instance [7], Lem. 3.10), which implies that equation (3.2) holds a.e. on I_1 . The same argument on \bar{p}_v instead of p_v shows that equation (3.2) holds a.e. on I_2 too, and so on I . This concludes the proof of Point 2. \square

Lemma 3.4. *Consider a subinterval (t_1, t_2) of $[0, t_f] \setminus I$. Then, $t \mapsto \langle q_r(t), d(t) \rangle$ is a nonincreasing function on (t_1, t_2) .*

In order to prove Lemma 3.4, we will show that $\langle q_r(t), d(t) \rangle$ is locally nonincreasing, i.e., for any $t_0 \in [0, t_f]$ and any $t > t_0$ close enough, there holds $\langle q_r(t), d(t) \rangle \leq \langle q_r(t_0), d(t_0) \rangle$. We first prove two preliminary lemmas.

Lemma 3.5. *For a.e. $t \in (t_1, t_2) \subset [0, t_f] \setminus I$, there holds*

$$\langle \dot{p}_v(t), \dot{d}(t) \rangle \geq 0.$$

Proof. Recall first (see Rem. 3.2), that $d(\cdot)$ is absolutely continuous on (t_1, t_2) and that on such an interval,

$$d(t) = \frac{p(t)}{\|p(t)\|} \quad \text{or} \quad d(t) = \left(\sin(\theta) \frac{\bar{p}_v(t)}{\|\bar{p}_v(t)\|}, \cos(\theta) \right).$$

Thus, for a.e. $t \in (t_1, t_2)$, we have either

$$\langle \dot{p}_v(t), \dot{d}(t) \rangle = \frac{1}{\|p_v(t)\|} \left(\|\dot{p}_v(t)\|^2 - \frac{\langle \dot{p}_v(t), p_v(t) \rangle^2}{\|p_v(t)\|^2} \right),$$

or,

$$\langle \dot{p}_v(t), \dot{d}(t) \rangle = \frac{\sin(\theta)}{\|\bar{p}_v(t)\|} \left(\|\dot{\bar{p}}_v(t)\|^2 - \frac{\langle \dot{\bar{p}}_v(t), \bar{p}_v(t) \rangle^2}{\|\bar{p}_v(t)\|^2} \right).$$

Both expressions are nonnegative due to Cauchy-Schwarz inequality. \square

Note that moreover $\langle \dot{p}_v(t), \dot{d}(t) \rangle = 0$ if and only if $p_v(t)$ and $\dot{p}_v(t)$ are collinear when $d(t) = \frac{p(t)}{\|p(t)\|}$, and if and only if $\bar{p}_v(t)$ and $\dot{\bar{p}}_v(t)$ are collinear otherwise.

Corollary 3.6. *If the state constraint is not active (i.e. $h(r(t)) \neq 0$) on $(t_1, t_2) \subset [0, t_f] \setminus I$, then $\langle q_r(t), d(t) \rangle$ is differentiable a.e. on (t_1, t_2) and*

$$\frac{d}{dt} \langle q_r(t), d(t) \rangle \leq 0.$$

Moreover this derivative is zero if and only if $p_v(t)$ and q_r are collinear when $d(t) = \frac{p_v(t)}{\|p_v(t)\|}$, and if and only if $\bar{p}_v(t)$ and \bar{q}_r are collinear otherwise.

Proof. On (t_1, t_2) , the measure μ is zero, so that q_r is constant and $\dot{p}_v(t) = -q_r$. Therefore, the sign of the derivative

$$\frac{d}{dt} \langle q_r(t), d(t) \rangle = \langle q_r, \dot{d}(t) \rangle = -\langle \dot{p}_v(t), \dot{d}(t) \rangle$$

is given by Lemma 3.5. \square

Lemma 3.7. *Let $(t_1, t_2) \subset [0, t_f] \setminus I$ and let $t_0 \in (t_1, t_2)$ be such that $h(r(t_0)) = 0$. Then*

$$\langle n(t_0), d(t_0) \rangle > 0, \quad \text{where } n(t) = \begin{pmatrix} -\tan(\gamma) \frac{\bar{r}(t)}{\|\bar{r}(t)\|} \\ 1 \end{pmatrix}.$$

Proof. Set $h[t] = h(r(t))$. Since $h(r) = r_z - \tan(\gamma)\|\bar{r}\|$, the function $t \mapsto h[t]$ is C^1 at times such that $\bar{r}(t) \neq 0$. Its derivative

$$\dot{h}[t] = \langle n(t), v(t) \rangle,$$

is absolutely continuous and, for a.e. t ,

$$\ddot{h}[t] = \frac{T}{m(t)} \|u(t)\| \langle n(t), d(t) \rangle - g_0 + \langle \dot{n}(t), v(t) \rangle. \quad (3.3)$$

Moreover, due to Cauchy-Schwarz inequality, we have

$$\langle \dot{n}(t), v(t) \rangle = \frac{\tan(\gamma)}{\|\bar{r}(t)\|} \left(-\|\bar{v}(t)\|^2 + \frac{\langle \bar{r}(t), \bar{v}(t) \rangle^2}{\|\bar{r}(t)\|^2} \right) \leq 0. \quad (3.4)$$

Note that the argument in Remark 2.4 shows that $\bar{r}(t_0) \neq 0$ if $\gamma \neq 0$, so the expression above is well-defined and $\dot{h}[t]$ is differentiable at t_0 .

Since $h[t] \geq 0$ on $[0, t_f]$, t_0 is a minimum of $h[t]$, therefore $\dot{h}[t_0] = 0$. Moreover, there exists a sequence of times $t^k > t_0$ converging to t_0 such that $\dot{h}[t^k] \geq 0$. Thus

$$\int_{t_0}^{t^k} \ddot{h}[t] dt = \dot{h}[t^k] \geq 0.$$

Using equations (3.3) and (3.4), this implies

$$\int_{t_0}^{t^k} \frac{T}{m(t)} \|u(t)\| \langle n(t), d(t) \rangle dt \geq g_0(t^k - t_0).$$

The function $d(t)$ being continuous (see Rem. 3.2), $\langle n(t), d(t) \rangle$ is continuous too, and the above inequality implies that $\langle n(t_0), d(t_0) \rangle$ is nonnegative and then

$$g_0 \leq \frac{1}{t^k - t_0} \int_{t_0}^{t^k} \frac{T}{m(t)} \|u(t)\| \langle n(t), d(t) \rangle dt \leq \frac{T}{m_e} u_{\max} \max_{[t_0, t^k]} \langle n(t), d(t) \rangle,$$

and $\max_{[t_0, t^k]} \langle n(t), d(t) \rangle$ tends toward $\langle n(t_0), d(t_0) \rangle$ when t^k converges to t_0 , which gives the result. \square

Remark 3.8. The above inequality shows also that if $\|u(t)\|$ has a limit α when t tends toward t_0 , then the limit α satisfies $T\alpha \geq m_e g_0 \cos(\gamma)$.

Proof of Lemma 3.4. Let $t_0 \in [0, t_f]$. If $h[t_0] \neq 0$, then $h[t] \neq 0$ in a neighborhood of t_0 . It then results from Corollary 3.6 that $t \mapsto \langle q_r(t), d(t) \rangle$ is nonincreasing near t_0 .

We are left with the case $h[t_0] = 0$. Recall that, for $t > t_0$, we have from the maximum principle

$$q_r(t) = q_r(t_0) - \int_{[t_0, t]} n(s) \mu(ds),$$

and that the function $d(\cdot)$ is absolutely continuous on (t_1, t_2) , so that, for t near t_0 , $d(t) - d(t_0) = \int_{t_0}^t \dot{d}(s) ds$. Thus, for $t > t_0$ close enough to t_0 we have

$$\langle q_r(t), d(t) \rangle - \langle q_r(t_0), d(t_0) \rangle = I_1 + I_2 - I_3, \quad (3.5)$$

where

$$I_1 = \int_{t_0}^t \langle q_r(s), \dot{d}(s) \rangle ds, \quad I_2 = \int_{t_0}^t \left\langle \int_{[t_0, s]} n(\sigma) \mu(d\sigma), \dot{d}(s) \right\rangle ds, \\ I_3 = \int_{[t_0, t]} \langle n(s), d(t) \rangle \mu(ds).$$

First, by Lemma 3.5 we have $I_1 \leq 0$. Second, $p_v(t)$ and $q_r(t)$ are bounded near t_0 , and so $\dot{d}(t)$ is bounded too. Since μ is a positive measure, we obtain

$$I_2 \leq (t - t_0) Cst \int_{[t_0, t]} \mu(ds).$$

Third, by Lemma 3.7 and the continuity of $\langle n(t), d(t) \rangle$, we obtain

$$I_3 \geq \frac{1}{2} \langle n(t_0), d(t_0) \rangle \int_{[t_0, t]} \mu(ds).$$

As a consequence, $I_2 - I_3 \leq 0$ for $t - t_0$ small enough. Thus $\langle q_r(t), d(t) \rangle \leq \langle q_r(t_0), d(t_0) \rangle$ for $t > t_0$ close enough to t_0 , which concludes the proof. \square

Proof of Proposition 3.3-Point 3. Let us show that for every $t_0 \in [0, t_f]$, $t \mapsto \langle q_r, d \rangle$ is nonincreasing almost everywhere in the neighbourhood of t_0 . If equation (3.1) is true at t_0 , the result is given by Lemma 3.4. Otherwise, let us consider the case when $\bar{p}_v(t_0) = 0$ and $p_{v_z}(t_0) < 0$. The case when $p_v(t_0) = 0$ can be treated in the same way. Firstly, it should be noted that

1. from $q_z(t) = p_z(t_0) - \int_{[0, t]} \mu(ds)$, q_z is a nonincreasing function on $[0, t_f]$;
2. from $\bar{q}_r(t) = \bar{p}_r(t_0) + \int_{[0, t]} \tan(\gamma) \frac{\bar{r}}{\|\bar{r}\|} \mu(ds)$, as $\bar{r}(t_0) \neq 0$ if $h(t_0) = 0$ and q_r is constant if $h(t_0) \neq 0$, q_x and q_y are monotonous in a neighbourhood of t_0 ;
3. $\bar{p}_v(t) = - \int_{t_0}^t \bar{q}_r(s) ds$.

Recall that we denote by \bar{d} the vector composed of the two first coordinates of d . Then, in a neighbourhood (t_-, t_+) of t_0 , with $t_- \leq t_+$,

$$\langle q_r, d \rangle = \langle \bar{q}_r, \bar{d} \rangle + \cos(\theta) q_z.$$

As q_z is nonincreasing, let us show that $\langle \bar{q}_r, \bar{d} \rangle$ is nonincreasing. From 2. on each interval $J = (t_-, t_0)$ or (t_0, t_+) ,

- either $\bar{q}_r = 0$ and $\langle \bar{q}_r, \bar{d} \rangle = 0$ is constant;
- or $\bar{q}_r(t) \neq 0 \forall t \in J$, thus $\bar{p}_v(t) \neq 0$ and $\bar{d} = \sin(\theta) \frac{\bar{p}_v}{\|\bar{p}_v\|}$. In this case,

$$\langle \bar{q}_r, \bar{d} \rangle = - \frac{\sin(\theta)}{\|\bar{p}_v(t)\|} \int_{t_0}^t \langle \bar{q}_r(s), \bar{q}_r(t) \rangle ds.$$

We can assume, by reducing the interval J if necessary, that for every t and s in J , $\text{sign}(q_x(t)) = \text{sign}(q_x(s))$ and $\text{sign}(q_y(t)) = \text{sign}(q_y(s))$. It implies that $\langle \bar{q}_r(s), \bar{q}_r(t) \rangle \geq 0$, and then $\langle \bar{q}_r, \bar{d} \rangle$ is nonincreasing on J and is of the same sign as $(t_0 - t)$.

Combining these results, we obtain that $\langle \bar{q}_r, \bar{d} \rangle$ is nonincreasing on $(t_-, t_0) \cup (t_0, t_+)$, which concludes the proof of the proposition. \square

Proof of Theorem 1.1. Consider an optimal trajectory on $[0, t_f]$. From Lemma 3.1, the norm of the control has the following expression depending on the sign of Ψ :

$$\|u(t)\| = \begin{cases} u_{\max} & \text{if } \Psi(t) > 0, \\ u_{\min} & \text{if } \Psi(t) < 0. \end{cases}$$

Moreover the control is singular on an interval if $\Psi(t) = 0$ on this interval. Let us show that Ψ can change of sign at most two times or be constantly zero on at most one interval.

First, we study the sign of $\dot{\Psi}$ thanks to Proposition 3.3. Indeed, from Proposition 3.3-Point 2, the sign of the derivative of Ψ is the opposite of the one of $\langle q_r, d \rangle$. Moreover, from Proposition 3.3-Point 3, $\langle q_r, d \rangle$ is nonincreasing, thus it may be zero on at most one interval denoted $[\bar{t}_1, \bar{t}_2] \subset [0, t_f]$. Then, on $[0, \bar{t}_1)$, one has $\langle q_r, d \rangle > 0$, $\dot{\Psi} < 0$, and on $(\bar{t}_2, t_f]$ one has $\langle q_r, d \rangle < 0$, $\dot{\Psi} > 0$.

Now, let us detail the study of Ψ on the interval $[\bar{t}_1, \bar{t}_2]$. Assume first that $\Psi(t) \neq 0$ for every $t \in [\bar{t}_1, \bar{t}_2]$. Then, on $[0, \bar{t}_1]$ (respectively $[\bar{t}_2, t_f]$) as Ψ is continuous from Proposition 3.3-Point 1 and decreasing (resp. increasing), it may be zero at most one time. Finally on $[0, t_f]$ it may be zero and change of sign at most two times. If $\Psi(t) > 0$ on $[\bar{t}_1, \bar{t}_2]$, then Ψ is strictly positive everywhere on $[0, t_f]$. If $\Psi(t) < 0$ on $[\bar{t}_1, \bar{t}_2]$, let us define $t_1 \in [0, \bar{t}_1)$ (resp. $t_2 \in (\bar{t}_2, t_f]$) such that $\Psi(t_1) = 0$ or $t_1 = 0$ (resp. $t_2 = t_f$). Then $\Psi(t) > 0$ on $[0, t_1) \cup (t_2, t_f]$ and $\Psi(t) < 0$ on (t_1, t_2) . Note that $\langle q_r, d \rangle(0) < 0$ corresponds to selecting $t_1 = 0$.

Assume now that Ψ crosses zero on $[\bar{t}_1, \bar{t}_2]$. As $\dot{\Psi}(t)$ is zero on that interval, then $\Psi(t) = 0$ for all $t \in [\bar{t}_1, \bar{t}_2]$. Moreover, as it is decreasing on $[0, \bar{t}_1]$ and increasing on $[\bar{t}_2, t_f]$, we obtain $\Psi(t) > 0$ for all $t \in [0, \bar{t}_1) \cup (\bar{t}_2, t_f]$.

This study on the sign of Ψ ends the proof of the theorem. \square

3.3. Structure of the optimal control when considering the effect of the atmosphere

The structure of optimal controls described in Theorem 1.1 seems to be preserved when one take into account the effect of an atmosphere. It has been proven in [14] for a simple one-dimensional dynamics. We will extend the result to our framework but with a simplified model of the effect of the atmosphere at low altitude. Indeed, we model this effect by applying an additional force in the direction of the launcher, which introduces a new term $\frac{\sigma}{m\|u\|}u$ in the equation of \dot{v} . The new dynamics is given by

$$\begin{cases} \dot{r} & = v, \\ \dot{v} & = \left(T - \frac{\sigma}{\|u\|}\right) \frac{u}{m} - g, \\ \dot{m} & = -q\|u\|, \end{cases} \quad (3.6)$$

where σ is a constant parameter which depends on the engine nozzle exit area and on the atmospheric pressure assumed to be constant with respect to altitude. We make the following assumption.

Assumption 3.9. The net thrust is always positive: $Tu_{\min} \geq \sigma$.

Also, for the sake of simplicity, we do not consider here the pointing constraint (but we keep the glide-slope constraint). Finally, the optimal control problem is formulated as follows.

Problem 3.10.

$$\min \ell(t_f, X(t_f)) \text{ such that}$$

$$\begin{cases} X(\cdot) = (r(\cdot), v(\cdot), m(\cdot)) \text{ follows equation (3.6),} \\ X(0) = (r_0, v_0, m_0), \\ (z, v_z)(t_f) = (0, 0), \\ m(t) > m_e \quad \forall t \in [0, t_f], \\ u_{\min} \leq \|u\| \leq u_{\max}. \end{cases}$$

We are able to prove that the optimal trajectories of this problem have the same structure as the ones of Problem 2.1.

Theorem 3.11. *Consider an optimal trajectory on $[0, t_f]$ of Problem 3.10. Then, the control $u(t)$ is in the Max-Min-Max or the Max-Singular-Max form, i.e. there exist t_1 and t_2 with $0 \leq t_1 \leq t_2 \leq t_f$ such that*

$$\|u\|(t) = \begin{cases} u_{\max} & \text{if } t \in [0, t_1] \cup (t_2, t_f], \\ u_{\min} \text{ or singular} & \text{if } t \in [t_1, t_2]. \end{cases}$$

The proof of this results follows the lines as the one of Theorem 1.1, so we only detail here the changes. Consider the Hamiltonian of Problem 3.10,

$$H(X, P, u) = \langle p_r, v \rangle + \left\langle p_v, \left(T - \frac{\sigma}{\|u\|} \right) \frac{u}{m} - g \right\rangle - p_m q \|u\|.$$

The dynamics of the adjoint vector is

$$\begin{cases} \dot{p}_r(t) &= 0, \\ \dot{p}_v(t) &= -q_r(t), \\ \dot{p}_m(t) &= \frac{1}{m(t)^2} \left\langle p_v(t), \left(T - \frac{\sigma}{\|u(t)\|} \right) u(t) \right\rangle. \end{cases} \quad (3.7)$$

Lemma 3.12. *Every optimal control of Problem 3.10 satisfies*

$$\|u(t)\| = \begin{cases} u_{\max} & \text{if } \Psi(t) > 0, \\ u_{\min} & \text{if } \Psi(t) < 0, \end{cases}$$

where

$$\Psi(t) = \frac{T}{m(t)} \|p_v(t)\| - p_m(t)q,$$

and, for all t such that $u(t) \neq 0$,

$$\frac{u(t)}{\|u(t)\|} = \frac{p_v(t)}{\|p_v(t)\|}.$$

Proof. If $u(\cdot)$ is an optimal control on $[0, t_f]$, then the maximization condition of the Pontryagin Principle implies that, for almost all $t \in [0, t_f]$, $u(t)$ maximizes

$$\varphi(t, w) = \left\langle p_v, \left(T - \frac{\sigma}{\|w\|} \right) \frac{w}{m} \right\rangle - p_m q \|w\|$$

among all $w \in \mathcal{U}$. Making the change of variable $w = \alpha d$, with $\alpha = \|w\|$, to find $u(t) \in \mathcal{U}$ maximizing φ amounts to find α and d maximizing

$$\varphi(t, \alpha, d) = \alpha \left(\frac{T}{m} \langle p_v, d \rangle - p_m q \right) - \frac{\sigma}{m} \langle p_v, d \rangle,$$

under the conditions $u_{\min} \leq \alpha \leq u_{\max}$ and $d \in \mathcal{S}^2$. It is clear that this maximization yields to the statement of the lemma. □

Lemma 3.13. *Consider an optimal trajectory on $[0, t_f]$. Then:*

1. Ψ is absolutely continuous on $[0, t_f]$;
2. $t \mapsto \left\langle q_r(t), \frac{p_v(t)}{\|p_v(t)\|} \right\rangle$ is a nonincreasing function on a full measurement subset of $[0, t_f]$.

Proof. We do not detail the proof here as it is very similar to the one of Proposition 3.3-Points 1,3. □

Proof of Theorem 3.11. Let study the sign of $\Psi(t)$. Its derivative is expressed by

$$\dot{\Psi}(t) = \frac{1}{m(t)} \left(\frac{\sigma q}{m(t)} \|p_v\| - T \left\langle q_r(t), \frac{p_v(t)}{\|p_v(t)\|} \right\rangle \right),$$

and can be written as follows

$$\dot{\Psi}(t) = K(t)\Psi(t) + \frac{1}{m(t)} f(t),$$

where K and f are functions expressed by

$$K(t) = \frac{\sigma q}{Tm(t)} \quad \text{and} \quad f(t) = \frac{\sigma q^2}{T} p_m(t) - T \left\langle q_r(t), \frac{p_v(t)}{\|p_v(t)\|} \right\rangle.$$

We deduce that

$$\frac{d}{dt} \left[\Psi(t) e^{-\int_0^t K(s) ds} \right] = \frac{e^{-\int_0^t K(s) ds}}{m(t)} f(t).$$

Using the expression of the optimal control given in Lemma 3.12 and from equation (3.7), we obtain that the derivative of p_m is expressed by $\frac{\|p_v\|}{m(t)^2} (T\|u\| - \sigma)$; therefore, from Assumption 3.9, $\dot{p}_m(t) > 0$ and p_m is increasing. By Lemma 3.13 the function $\left\langle q_r(t), \frac{p_v(t)}{\|p_v(t)\|} \right\rangle$ is nonincreasing, thus we obtain that $f(t)$ is increasing and can change of sign at most one time. Consequently, $\Psi(t) e^{-\int_0^t K(s) ds}$ can changes of sign at most two times, and in that case it is positive, then negative and then positive, and Ψ has the same property. □

4. ADDITIONAL PROPERTIES OF OPTIMAL TRAJECTORIES

Optimal trajectories may contain two kind of arcs that play a very specific role both from a theoretical and numerical point of view: singular arcs, on which the value of the control is not determined by the maximisation of the Hamiltonian, and boundary arcs, where the state constraint is active. The aim of this section is to study the occurrence of such phenomena. We will obtain results mainly in the particular case where the glide-slope constraint reduces to an altitude constraint, *i.e.* the case where $\gamma = 0$.

4.1. Singular arcs

A *singular arc* is the restriction of an optimal trajectory to an interval $(t'_1, t'_2) \subset [0, t_f]$ on which the switching function Ψ is zero. From Theorem 1.1, optimal trajectories may contain a singular arc, but not more than one.

In the study of singular arcs we present below, we first give two lemmas showing that such arcs have a particular form, namely some adjoint vectors are collinear and the pointing constraint is active. Then we show in Proposition 4.4 that in the case $\gamma = 0$, these properties happen only if the initial conditions are in very specific positions, so that singular arcs do not appear for generic initial conditions. We did not try to extend the result to $\gamma \neq 0$, but it is reasonable to believe that the results (no singular arc for generic initial conditions) still hold in these case.

Lemma 4.1. *Consider an optimal trajectory on $[0, t_f]$. Assume that it contains a singular arc defined on an interval $(t'_1, t'_2) \subset [0, t_f] \setminus I$. Then there holds*

$$\int_{[t'_1, t'_2]} \mu(ds) = 0. \quad (4.1)$$

Moreover if the pointing constraint is not active (i.e. $d(t) = \frac{p_v(t)}{\|p_v(t)\|}$), then $p_v(t)$ and $q_r(t)$ are collinear, otherwise $\bar{p}_v(t)$ and $\bar{q}_r(t)$ are collinear.

Remark 4.2. Equation (4.1) means either that the state constraint (i.e. the glide-slope constraint) is never active, or that on each open interval where this constraint is active, the adjoint vector follows the same equations as when the constraint is not active. However a singular part of the measure μ at t'_2 is not excluded.

Proof. Since $\Psi(t) = 0$ on (t'_1, t'_2) , there holds $\dot{\Psi}(t) = 0$ a.e. on (t'_1, t'_2) , and it follows from Proposition 3.3 that $\langle q_r(t), d(t) \rangle$ is constantly equal to zero on (t'_1, t'_2) . If the state constraint is not active on (t'_1, t'_2) , the conclusion follows from Corollary 3.6. If the constraint is active at some time $t'_0 \in (t'_1, t'_2)$, following the lines of the proof of Lemma 3.4, we obtain from equation (3.5) that both I_1 and $I_2 - I_3$ must be zero near t'_0 . The latter implies

$$\langle n(t'_0), d(t'_0) \rangle \int_{[t'_0, t]} \mu(ds) = 0$$

which again gives the conclusion since $\langle n(t'_0), d(t'_0) \rangle > 0$ by Lemma 3.7. \square

Lemma 4.3. *If the pointing constraint is not active on an interval $(t'_1, t'_2) \subset [0, t_f] \setminus I$, then the trajectory is not singular on that interval.*

Proof. If the trajectory is singular (t'_1, t'_2) , then by Lemma 4.1, q_r and p_v are collinear on this interval. Moreover, when the pointing constraint is not active, $\dot{\Psi} = 0$ implies from equation (3.2) that $\langle q_r, d \rangle = \frac{\langle q_r, p_v \rangle}{\|p_v\|} = 0$. Thus $q_r = 0$. Now, from equation (2.3), which is equivalent to

$$H(X, P, u) = \|u\| \Psi + \langle q_r, v \rangle - p_{v_z} g_0,$$

the expression of the Hamiltonian becomes

$$H(X, P, u) = -p_{v_z} g_0.$$

The transversality condition (2.5) and the condition (2.2) on ℓ then imply that $p_{v_z} \leq 0$, which contradicts the assumption that the pointing constraint is not active. \square

Consider now the particular case where the glide-slope constraint reduces to an altitude constraint, i.e. the case where $\gamma = 0$. In that case, $n = e_z$, so $\bar{q}_r = \bar{p}_r$ is constant even when $h(r) = 0$. Moreover we impose that the final position and velocity are fixed and null, i.e. we choose as target $\mathcal{C} = \{X \in \mathbb{R}^7 : r = v = 0\}$.

Proposition 4.4. *Under the above assumptions, if the optimal trajectory contains a singular arc, then the initial conditions are such that $(x, y)(0)$ and $(v_x, v_y)(0)$ are collinear. Consequently, for generic initial conditions there are no singular arcs.*

Proof. Consider a trajectory containing a singular arc on an interval $[t'_1, t'_2]$. According to Lemma 4.1, $\bar{p}_v(t'_1)$ and \bar{p}_r are collinear. Set $\bar{d} = (d_x, d_y)$, $\bar{r} = (x, y)$ and $\bar{v} = (v_x, v_y)$. Since $(r(t_f), v(t_f)) = (0, 0)$, \bar{d} has the same direction as \bar{p}_v and as $\dot{\bar{v}}$ by the dynamics of the vehicle. We conclude that $\bar{r}(0)$ and $\bar{v}(0)$ are collinear. \square

Proposition 4.4 helps to explain why singular trajectories seldom arise in numerical simulations and are often dismissed in the literature. Note that we make additional assumptions in order to give a simple proof but the results could probably be extended, for example by continuity arguments.

Remark 4.5. The condition $(x, y)(0)$ and $(v_x, v_y)(0)$ linearly dependent is satisfied for instance when considering the two dimensional problem, which has been studied many times in the literature. Thus, it seems that singular arcs appear rarely. From our own observations, the most common cases where they appear seem to be when the cost depends on the final time and q is small (the mass varies slightly).

4.2. Number of contact points

Given a trajectory, we say that $[t_{c_1}, t_{c_2}]$ is a *boundary interval* if $h(t) = 0$ for all $t \in [t_{c_1}, t_{c_2}]$, and $[t_{c_1}, t_{c_2}]$ is the largest interval satisfying this condition and containing t_{c_1}, t_{c_2} . When the boundary interval is reduced to a point t_c (i.e. $t_{c_1} = t_{c_2} = t_c$), we rather say that t_c is a *contact point*.

The aim of this subsection is to show that there are few boundary intervals along an optimal trajectory in general. To keep the problem manageable we restrict ourselves to the particular setting where:

- the state constraint reduces to an altitude constraint (i.e. $\gamma = 0$), as in the end of the previous subsection; remind that in that case $n = e_z$, so $\bar{q}_r = \bar{p}_r$ is constant even when $h(r) = 0$;
- the mass m is assumed to be constant, i.e. $q = 0$.

Lemma 4.6. *There is at most one contact point or boundary interval on each Max or Min arc of an optimal trajectory.*

Proof. Let us show that there is at most one contact point or boundary interval on each Max arc (including possibly the final point for the last Max arc). A similar reasoning on Min arcs will then give the conclusion. By contradiction, assume that the same Max arc contains two different boundary intervals $[t'_{c_1}, t_{c_1}]$ and $[t_{c_2}, t'_{c_2}]$, with $t_{c_1} < t_{c_2}$. We can moreover assume that $h(t) = z(t) > 0$ on (t_{c_1}, t_{c_2}) . Then

$$\dot{v}_z(t_{c_1}) \geq 0, \quad \dot{v}_z(t_{c_2}) \geq 0,$$

and there exists $t_b \in (t_{c_1}, t_{c_2})$ such that $\dot{v}_z(t_b) < 0$.

Note that \dot{v}_z is an affine function of d_z , the vertical component of d ,

$$\dot{v}_z = u_{\max} \frac{T}{m} d_z - g_0,$$

so the above sign condition on \dot{v}_z write as

$$d_z(t_{c_1}) \text{ and } d_z(t_{c_2}) \geq \frac{mg_0}{Tu_{\max}}, \quad d_z(t_b) < \frac{mg_0}{Tu_{\max}}. \quad (4.2)$$

Now, on (t_{c_1}, t_{c_2}) , the state constraint is inactive, therefore $q_r = q_r(t_{c_1})$ is constant and

$$p_v(t) = p_0 - q_r t, \quad \forall t \in (t_{c_1}, t_{c_2}).$$

Assume first that p_0 and q_r are collinear, and write $p_0 = \rho_0 \delta$ and $q_r = \rho_r \delta$, with $\rho_0, \rho_r \in \mathbb{R}$ and $\delta \in \mathcal{S}^2$. Thus,

$$\frac{p_v}{\|p_v\|} = \text{sign}(\rho_0 - \rho_r t) \delta.$$

We deduce that in that case d_z can take only two values, $\cos(\theta)$ and the constant value $|\delta_z|$ (if this value belongs to $(\cos(\theta), 1]$), and can change value at most one time. This contradicts equation (4.2).

Thus p_0 and q_r are not collinear. In particular d is absolutely continuous on (t_{c_1}, t_{c_2}) . First, let us notice that when the pointing constraint is active, d_z is constantly equal to $\cos(\theta)$, and study now the evolution of d_z when the pointing constraint is not active. We will reduce the problem to two dimensions. Let us choose $\hat{n} = \pm \frac{p_0 \wedge q_r}{\|p_0 \wedge q_r\|}$ such that $\langle \hat{n}, e_z \rangle \geq 0$. Then d , which is equal to $\frac{p_v}{\|p_v\|}$, belongs to the normal plane to \hat{n} , denoted \hat{n}^\perp . Note that $\hat{n} \neq e_z$. Indeed, otherwise $p_{v_z} = 0$, which implies that d_z is constantly equal to $\cos(\theta)$ and is in contradiction with equation (4.2). Let α be the angle between \hat{n} and the plane (e_x, e_y) and let us choose (u_1, u_2) an orthonormal basis of \hat{n}^\perp such that $\langle u_1, e_z \rangle = 0$ and $\langle u_2, e_z \rangle = \cos(\alpha) > 0$. Then, we define ϕ such that d can be written

$$d = \cos(\phi)u_1 + \sin(\phi)u_2$$

with $\phi \in [-\frac{\pi}{2}, \frac{\pi}{2}]$ and we have that

$$d_z = \sin(\phi) \cos(\alpha).$$

We have from equation (4.2) that $\phi(t_{c_1})$ and $\phi(t_{c_2})$ are in $(0, \frac{\pi}{2})$. Now, let us show that the evolution of d_z contradicts equation (4.2). Since α is constant,

$$\dot{d}_z = \dot{\phi} \cos(\phi) \cos(\alpha), \tag{4.3}$$

therefore, \dot{d}_z has the same sign as $\dot{\phi}$, and $\dot{\phi}$ can be expressed thanks to the following computations. We reduce ourselves to \hat{n}^\perp , since p_v, p_0 and q_r belongs to it. We place ourselves in this plane in the coordinates defined by (u_1, u_2) . By abuse of notation, we will call p_v the vector in two dimensions defined by $p_v = (\langle p_v, u_1 \rangle, \langle p_v, u_2 \rangle)$. As $p_v = \|p_v\| d = \|p_v\| \begin{pmatrix} \cos(\phi) \\ \sin(\phi) \end{pmatrix}$, then

$$\dot{p}_v = \frac{d\|p_v\|}{dt} \begin{pmatrix} \cos(\phi) \\ \sin(\phi) \end{pmatrix} + \|p_v\| \dot{\phi} \begin{pmatrix} -\sin(\phi) \\ \cos(\phi) \end{pmatrix},$$

and by multiplying on the left by $(-\sin(\phi) \quad \cos(\phi))$ we obtain

$$\begin{pmatrix} -\sin(\phi) \\ \cos(\phi) \end{pmatrix}^T (-q_r) = \|p_v\| \dot{\phi}.$$

We deduce that

$$\dot{\phi} = -\frac{1}{\|p_v\|^2} \det(q_r, p_v) = -\frac{1}{\|p_v\|^2} \det(q_r, p_0).$$

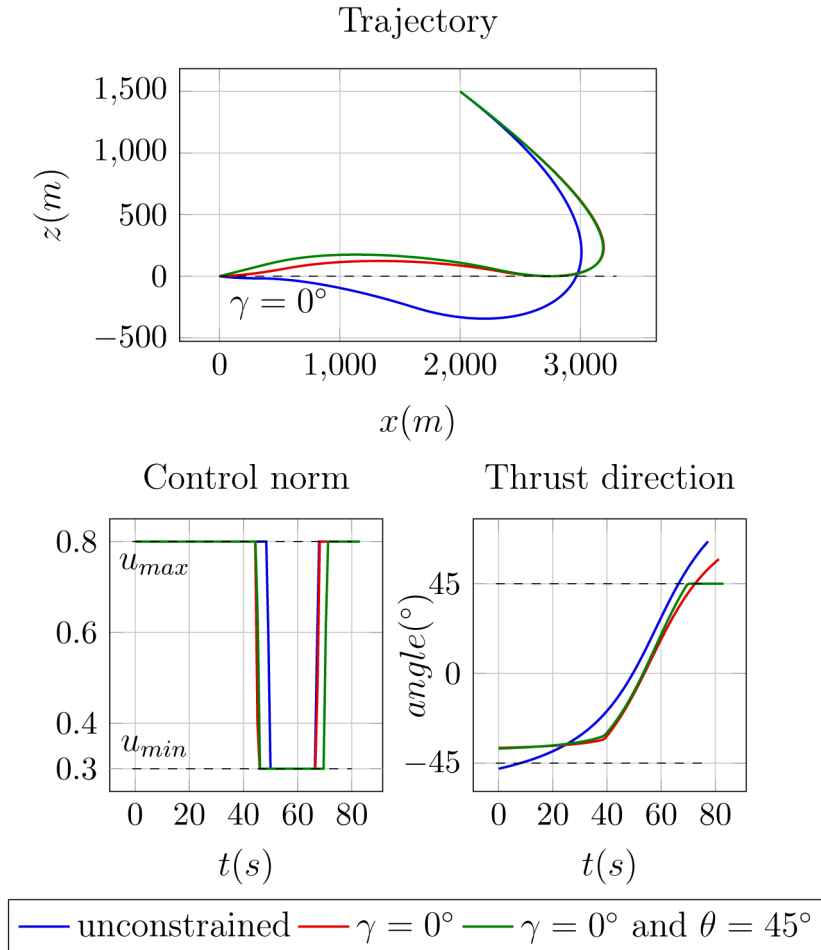


FIGURE 3. Simulation results for $q = 0$ without glide-slope or pointing constraint (blue), with only a glide-slope constraint of $\gamma = 0^\circ$ (red) and with glide-slope and pointing constraints for $\theta = 45^\circ$ (green).

As q_r and p_0 are constant, we deduce that $\dot{\phi}$ is of constant sign, and \dot{d}_z also from equation (4.3). Thus, d_z is monotonous when the pointing constraint is not active and constant when it is active: we conclude that it is not possible to verify equation (4.2). □

Corollary 4.7. *For generic initial conditions, there are at most three contact points or boundary intervals along an optimal trajectory. More precisely,*

1. if $u_{\min} < \frac{m_0 g_0}{T}$, there is along the trajectory at most two contact points or boundary intervals;
2. if $u_{\min} \cos(\theta) \geq \frac{m_0 g_0}{T}$, the only possible contact point is the final point.

Proof. The main statement follows by application of Theorem 1.1 and Proposition 4.4, which imply that the control is of the form Max-Min-Max (or the restriction of such a control to a subinterval), and Lemma 4.6 gives us the number of contacts. Then, the assumption of Point 1 implies that $u_{\min} T$ does not compensate the weight of the vehicle, therefore it is not possible to have a contact on a Min arc without violating the state

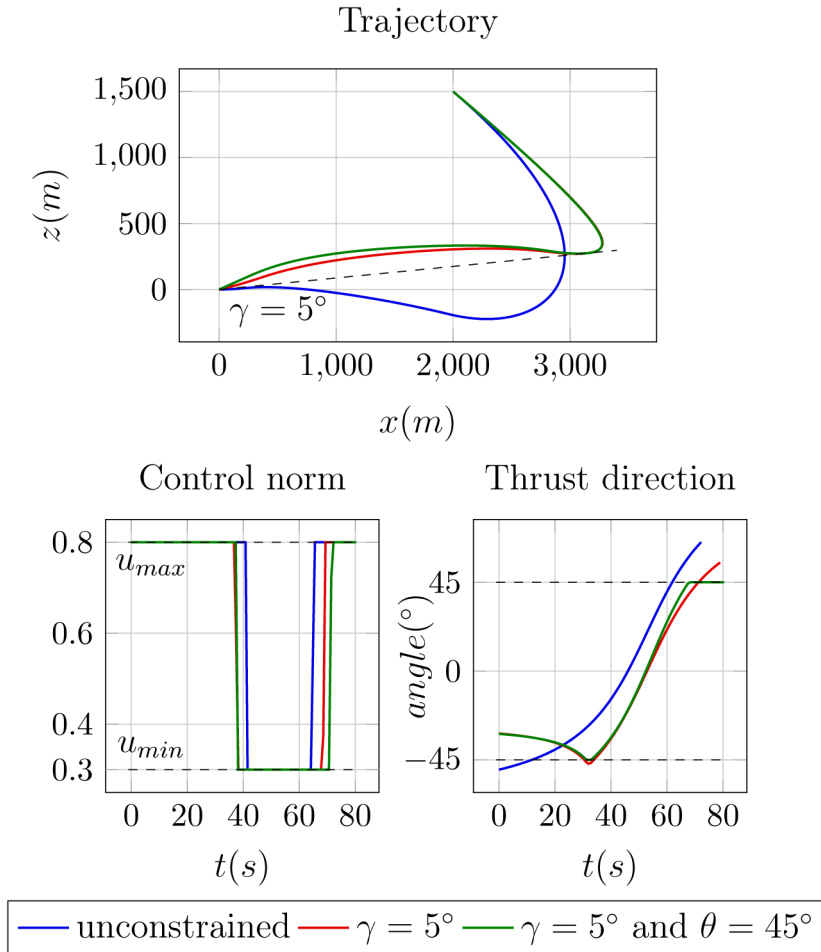


FIGURE 4. Simulation results with a varying mass, and a glide-slope constraint of $\gamma = 5^\circ$.

constraint. Finally, the assumption of Point 2 implies that $u(t)T$ compensate the weight of the vehicle for any control direction, therefore the vertical velocity, and so the altitude, would remain positive after a contact with the state constraint. We deduce that it is not possible to have a contact aside from the final point. \square

Remark 4.8. The last result is demonstrated under the assumption of a constant mass. However we expect it to stay true if the mass has small variations, *i.e.* if q is small. Indeed, the reasoning is still correct if $m(t_b) \sim m(t_{c_1})$ or $m(t_{c_2})$, therefore it is sufficient to assume that the mass varies only slightly between two contact points. Likewise, the same reasoning would work with a glide-slope constraint of $\gamma \neq 0$, by assuming that n is constant, which means in two dimensions that the trajectory stays in the same half-plane $x \geq 0$ or $x \leq 0$.

5. NUMERICAL RESULTS

This section presents some examples for a Mars powered descent problem, in two dimensions for the sake of simplicity. The simulations are carried out by using CasADi ([3]) with python language and the IPOPT solver. They are performed under the same conditions as in [2]. The launcher parameters are $T = 16573N$, $u_{\min} = 0.3$ and $u_{\max} = 0.8$ and $m_e = 1505kg$ and $g_0 = 3.71m/s^2$ corresponds to the Mars gravitational acceleration. The initial state is given by $r_0 = [2000, 1500]m$, $v_0 = [100, -75]m/s$ and $m_0 = 1905kg$, and the final time t_f is free.

The considered optimal control problem aims to perform a pinpoint landing by steering the vehicle to null final position and velocity. In this setting it is usual to minimize fuel consumption

$$J = \int_0^{t_f} \|u(t)\| dt.$$

When $q \neq 0$, this cost is equal to $(m(0) - m(t_f))/q$, hence it is actually a final cost (which represents the maximisation of final mass) and we recover an optimal problem in the form of Problem 2.1. When $q = 0$, J is not a final cost and so our preceding study do not directly apply. But it is straightforward to show that all results presented in Sections 3 and 4 remain valid.

The first set of simulations is performed in the conditions of Section 4 with a constant vehicle mass, *i.e.* with $q = 0$. Note that the assumption of the Point 1 of Corollary 4.7 $u_{\min} < \frac{m_0 g_0}{T}$ is verified.

Three simulations were performed. The first executes a Mars landing if no pointing and altitude constraint is applied. Figure 3 shows that in that case, the zero altitude is crossed. In the second simulation, an altitude constraint has been added. We see that, in accordance with the results of Corollary 4.7, there are two contact points with the state constraint along the trajectory: one during the first Bang arc and the final point. However, the angle of the thrust exceeds 45° at the end of the trajectory. Finally, in the third example, a pointing constraint of 45° is added. There are again two contacts with the state constraints, and the pointing constraint is active during the last 16s of the trajectory, which has the effect of making the trajectory more vertical.

A second set of simulations has been performed with a varying mass, with $q = 8.4294$ kg/s, considering a glide-slope constraint of $\gamma = 5^\circ$. In that case, the constraints are more compelling, as we see on the green plot on Figure 4 that the thrust direction is saturated by the pointing constraint on both its inferior and its superior bounds. There is still one contact point with the state constraint, although we leave the framework of Corollary 4.7. Remark that in all examples the form of the control is Max-Min-Max, and even the switching times vary little from one simulation to another.

APPENDIX A.

Lemma A.1. *The solutions of the maximization problem*

$$\max_d \langle p_v, d \rangle \quad \text{under the conditions} \quad \begin{cases} c_+(d) = \langle e_z, d \rangle - \cos(\theta) \geq 0, \\ c_1(d) = \langle d, d \rangle - 1 = 0, \end{cases}$$

are the vectors $d \in \mathcal{S}^2$ satisfying

$$d = \begin{cases} \frac{p_v}{\|p_v\|} & \text{if } p_{v_z} \geq \|p_v\| \cos(\theta) \text{ and } p_v \neq 0, \\ \left(\sin(\theta) \frac{\bar{p}_v}{\|\bar{p}_v\|}, \cos(\theta) \right) & \text{if } p_{v_z} < \|p_v\| \cos(\theta) \text{ and } \bar{p}_v \neq 0, \\ \left(\sin(\theta) \delta, \cos(\theta) \right) \text{ where } \delta \in \mathcal{S}^1 & \text{if } p_{v_z} < \|p_v\| \cos(\theta) \text{ and } \bar{p}_v = 0. \end{cases}$$

Proof. Set $f = \langle p_v, d \rangle$. Denoting by λ_+ and λ the Lagrange multipliers associated to the conditions c_+ and c_1 , the Karush-Kuhn-Tucker optimality conditions write as

$$\begin{cases} \nabla f(d) + \lambda \nabla c_1(d) + \lambda_+ \nabla c_+(d) = 0 \\ c_+(d) \geq 0, \quad c_1(d) = 0, \\ \lambda_+ c_+(d) = 0, \\ \lambda_+ \geq 0, \end{cases}$$

where the gradients are given by

$$\nabla f(d) = p_v, \quad \nabla c_1(d) = 2d, \quad \nabla c_+(d) = e_z.$$

Case 1: $c_+(d) > 0$. Then $\lambda_+ = 0$, $p_v + 2\lambda d = 0$, $\langle d, d \rangle = 1$, and we get the following alternative. Either $p_v = 0$ and then every $d \in \mathcal{S}^2$ is a maximum. Or $d = \epsilon \frac{p_v}{\|p_v\|}$ with $\epsilon = \pm 1$, and since d maximizes f , then $\epsilon = 1$.

Case 2: $c_+(d) = 0$. Then $d_z = \cos \theta$, $p_v + 2\lambda d + \lambda_+ e_z = 0$, $\langle d, d \rangle = 1$, and we get the following alternative. Either $p_v = p_{v_z} e_z$ (i.e. $\bar{p}_v = 0$) with $p_{v_z} \leq 0$, and in this case, choosing $\lambda_+ = -p_{v_z}$ we obtain that every d of the form $(\sin(\theta)\delta, \cos(\theta))$, with $\delta \in \mathcal{S}^1$, is maximum. Or $p_v + \lambda_+ e_z \neq 0$ and so $d = \epsilon \frac{p_v + \lambda_+ e_z}{\|p_v + \lambda_+ e_z\|}$ with $\epsilon = \pm 1$. In that case, $\epsilon(p_{v_z} + \lambda_+) = \|p_v + \lambda_+ e_z\| \cos(\theta)$ and

$$d = \begin{pmatrix} \frac{\epsilon p_{v_x}}{\|p_v + \lambda_+ e_z\|} \\ \frac{\epsilon p_{v_y}}{\|p_v + \lambda_+ e_z\|} \\ \frac{\epsilon p_{v_z}}{\|p_v + \lambda_+ e_z\|} \end{pmatrix} = \cos(\theta) \begin{pmatrix} \frac{p_{v_x}}{(p_{v_z} + \lambda_+)} \\ \frac{p_{v_y}}{(p_{v_z} + \lambda_+)} \\ 1 \end{pmatrix}.$$

As d is unit, we have

$$\|d\|^2 = 1 = \cos(\theta)^2 \left(1 + \frac{p_{v_x}^2 + p_{v_y}^2}{(p_{v_z} + \lambda_+)^2} \right) = \cos(\theta)^2 \left(1 + \frac{\|\bar{p}_v\|^2}{(p_{v_z} + \lambda_+)^2} \right).$$

We deduce that

$$\sin(\theta)^2 = \cos(\theta)^2 \frac{\|\bar{p}_v\|^2}{(p_{v_z} + \lambda_+)^2}, \quad \text{so} \quad \frac{\cos \theta}{(p_{v_z} + \lambda_+)} = \epsilon \frac{\sin \theta}{\|\bar{p}_v\|}.$$

Thus,

$$d = \begin{pmatrix} \epsilon \sin(\theta) \frac{p_{v_x}}{\|\bar{p}_v\|} \\ \epsilon \sin(\theta) \frac{p_{v_y}}{\|\bar{p}_v\|} \\ \cos(\theta) \end{pmatrix},$$

and the parameter ϵ is equal to $+1$ since d maximizes f . □

REFERENCES

- [1] B. Acikmese, J. Carson and L. Blackmore. Lossless convexification of the soft landing optimal control problem with non-convex control bound and pointing constraints. *IEEE Trans. Control Syst. Technol.* **21** (2013) 2104–2113.
- [2] B. Acikmese and S. Ploen, Convex programming approach to powered descent guidance for mars landing. *J. Guidance Control Dyn.* **30** (2007) 1353–1366.
- [3] J.A.E. Andersson, J. Gillis, G. Horn, J.B. Rawlings and M. Diehl, CasADi – a software framework for nonlinear optimization and optimal control. *Math. Program. Comput.* **11** (2019) 1–36.
- [4] L. Blackmore, Autonomous precision landing of space rockets. *The Bridge* **46** (2016) 15–20.
- [5] L. Blackmore, B. Aıkmee and D.P. Scharf, Minimum-landing-error powered-descent guidance for mars landing using convex optimization. *J. Guidance Control Dyn.* **33** (2010) 1161–1171.
- [6] Z. Chen, J.-B. Caillaud and Y. Chitour, L1-minimization for mechanical systems. *SIAM J. Control Optim.* **54** (2016) 1245–1265.
- [7] Y. Chitour, F. Jean and E. Trélat, Genericity results for singular curves. *J. Differ. Geom.* **73** (2006) 45–73.
- [8] F. Gazzola and E.M. Marchini, A minimal time optimal control for a drone landing problem. *ESAIM: COCV* **27** (2021) 99.
- [9] G. Leitmann, On a class of variational problems in rocket flight. *J. Aerospace Sci.* **26** (1959) 586–591.
- [10] C. Leparoux, B. Hérissé and F. Jean, Optimal planetary landing with pointing and glide-slope constraints. *2022 61th IEEE Conference on Decision and Control (CDC)*, 2022.
- [11] P. Lu, Propellant-optimal powered descent guidance. *J. Guidance Control Dyn.* **41** (2018) 813–826.

- [12] L. Ma, K. Wang, Z. Xu, Z. Shao, Z. Song and L.T. Biegler, Multi-point powered descent guidance based on optimal sensitivity. *Aerospace Sci. Technol.* **86** (2019) 465–477.
- [13] J. Meditch, On the problem of optimal thrust programming for a lunar soft landing. *IEEE Trans. Automatic Control* **9** (1964) 477–484.
- [14] H. Ménou, E. Bourgeois and N. Petit, Fuel-optimal program for atmospheric vertical powered landing. in *2021 60th IEEE Conference on Decision and Control (CDC)*, 2021, 6312–6319.
- [15] A. Miele, The calculus of variations in applied aerodynamics and flight mechanics. *Math. Sci. Eng.* **5** (1962) 99–170.
- [16] S. Ploen, B. Acikmese and A. Wolf, A comparison of powered descent guidance laws for mars pinpoint landing. In *AIAA/AAS Astrodynamics Specialist Conference and Exhibit*, August 2006.
- [17] H.M. Robbins, Optimality of intermediate-thrust arcs of rocket trajectories. *AIAA J.* **3** (1965) 1094–1098.
- [18] H. Schättler, The local structure of time-optimal trajectories in dimension three under generic conditions. *SIAM J. Control Optim.* **26** (1988) 899–918.
- [19] R. Sostaric and J. Rea, Powered descent guidance methods for the moon and mars. in *AIAA Guidance, Navigation, and Control Conference and Exhibit*, June 2005.
- [20] H.J. Sussmann, The structure of time-optimal trajectories for single-input systems in the plane: the general real analytic case. *SIAM J. Control Optim.* **25** (1967) 868–904.
- [21] U. Topcu, J. Casoliva and K. Mease, Fuel efficient powered descent guidance for mars landing. in *AIAA Guidance, Navigation, and Control Conference and Exhibit*, 2005.
- [22] U. Topcu, J. Casoliva and K.D. Mease, Minimum-fuel powered descent for mars pinpoint landing. *J. Spacecraft Rockets* **44** (2007) 324–331.
- [23] E. Trélat, Optimal control and applications to aerospace: Some results and challenges. *J. Optim. Theory Appl.* **154** (2012) 713–758.
- [24] R. Vinter, Optimal Control. Modern Birkhauser Classics. Springer, 2010.
- [25] A.A. Wolf, B. Acikmese, Y. Cheng, J. Casoliva, J.M. Carson and M.C. Ivanov, Toward improved landing precision on mars. in *2011 Aerospace Conference*, March 2011.
- [26] W.P. Ziemer, Modern real analysis, Vol. 278 of *Graduate Texts in Mathematics*, 2nd edn. Springer, Cham, 2017. With contributions by Monica Torres.

Subscribe to Open (S2O)

A fair and sustainable open access model



This journal is currently published in open access under a Subscribe-to-Open model (S2O). S2O is a transformative model that aims to move subscription journals to open access. Open access is the free, immediate, online availability of research articles combined with the rights to use these articles fully in the digital environment. We are thankful to our subscribers and sponsors for making it possible to publish this journal in open access, free of charge for authors.

Please help to maintain this journal in open access!

Check that your library subscribes to the journal, or make a personal donation to the S2O programme, by contacting subscribers@edpsciences.org

More information, including a list of sponsors and a financial transparency report, available at: <https://www.edpsciences.org/en/math-s2o-programme>